



# First results in the realization of the unit Watt in airborne sound

Katharina VOELKEL<sup>1</sup>; Christian BETHKE<sup>1</sup>; Spyros BREZAS<sup>1</sup>; Volker WITTSTOCK<sup>1</sup>

<sup>1</sup> Physikalisch-Technische Bundesanstalt Braunschweig, Germany

## ABSTRACT

Sound power - though a main quantity in acoustics - is not a traceable quantity to this day because a standard device for the realization of the unit watt has not been developed. Changing this is one goal of a research project funded by the European Metrology Research Programme (EMRP). Basis for the realization of the unit watt in airborne sound is an embedded oscillating solid body whose sound power output can be calculated using Rayleigh's integral with measured velocity distributions on the radiator surface. Ideally, the solid body moves as a rigid unit and acts as a monopole. However, measurements show that a uniform movement of the radiator surface is difficult to achieve. It will be investigated whether such a source can nevertheless be considered as a monopole and at which frequencies. Thus, analyses on the comparability of numerical and analytical data as well as an investigation of the dependency of uncertainties on discretization of the measured radiator surface will be presented. Calculations will be compared to sound powers determined from sound pressure measurements on an enveloping surface for further verification.

Keywords: Sound Power, Metrology, Traceability      I-INCE Classification of Subjects Number: 72.4

## 1. INTRODUCTION

In naming the properties of a sound source, its sound power output - describing the total amount of sound radiated by the source - is a major factor. In contrast to sound pressure or sound intensity, sound power does not depend on the distance from the source or its acoustic environment. Hence, sound power is considered to be a truly source characterizing quantity. As such, several EU directives call for the determination of sound power output in the labeling of machinery and consumer products (1, 2, 3). Consequently several internationally accepted methods of sound power determination have been developed (4, 5, 6, 7, 8). These methods employ the measurement of sound pressure levels in free (4), essentially free (5, 6), diffuse (7), or nearly diffuse fields (8). Using either the mean sound pressure over enveloping surfaces (free field) or an integration over a room volume with calculated energy densities (diffuse field), the sound power output of a source under test is determined.

One major commonality of all of these methods is their dependence on the sound field assumption. However, even high quality laboratory rooms do not provide perfect free or diffuse fields nowadays as described in (12). Sound power determinations that are less dependent on the sound field are available and based on sound intensity measurements (9, 10, 11). Yet, uncertainty estimates for results obtained with these methods are intransparent as there is no primary standard for sound intensity to this day. These deficiencies cause the problem that sound power levels determined by one method can show a systematic deviation in excess of 1 dB from the sound power levels determined by another method, where it is unclear which method is more appropriate for the situation (12).

For this reason a joint research project (JRP) funded by the European Metrology Research Program (EMRP) has been started aiming at investigating a new approach for sound power determination in order to realize the unit Watt in airborne sound. This contribution will give an overview over this project and report first results.

## 2. PROJECT OVERVIEW

As commonly known, the unit Watt is a derived quantity based on the SI units for mass, length, and time (Eq.1)

$$1W = 1 \frac{\text{kg m}^2}{\text{s}^3} \quad (1)$$

<sup>1</sup>katharina.voelkel@ptb.de

Hence, to qualify as a primary realization of this unit, measurements on a sound source under test have to yield values in the units of mass, length, or time. Post-calculation formulas of sound power can only contain these measurement data and quantities that are traceable to one of the seven SI units themselves. This is to ensure that all input data can be measured with precise uncertainties and that the uncertainty of the thus determined sound power in Watt can be given with high accuracy. The sound source whose sound power output is determined in this manner is called a primary standard.

The approach to establish such a primary standard for the EMRP project referenced above is the use of an embedded oscillating body. Establishing a grid of measurement points which are modeled as individual monopole sources that radiate into a hemi-free field and integrating over an enveloping surface, the resulting sound power output of this device can be obtained using the discretized Rayleigh's integral according to (13, 14) (Eq. 2).

$$P = \frac{\rho c}{2\pi} k^2 \left[ \sum_{i=1}^N v_i^2 S_i^2 + \sum_{i=1}^N \sum_{\substack{j=1 \\ j \neq i}}^N v_i v_j S_i S_j \frac{\sin(k d_{ij})}{k d_{ij}} \cos(\phi_i - \phi_j) \right] \quad (2)$$

Here  $N$  denotes the number of monopoles,  $\rho$  the density of air,  $c$  the speed of sound in air,  $k$  the wavenumber,  $v_i$  the measured velocity of the  $i$ -th element,  $S_i$  the assigned surface area of the  $i$ -th element,  $d_{ij}$  the distance between the  $i$ -th and  $j$ -th element, and  $\phi_i$  the measured phase of vibration of the  $i$ -th element.

It should be noted that the assumption of monopoles radiating into a hemi-free field excludes the possibility of using a loudspeaker as primary standard. The cone surrounding the membrane of a loudspeaker does not provide a hemispherical free field for every point on the membrane. This would be especially critical for the membrane boundary.

Hence, a flat oscillating body was chosen for the set-up. Its surface velocity can be measured for any frequency including phase using a laser scanning vibrometer with a user specified grid size. Each one of the measurement points can then be assigned a surface area value equal to the grid size at that measurement point (Fig. 1). Thus, measurement data do indeed only contain values in the units of length and time. All quantities

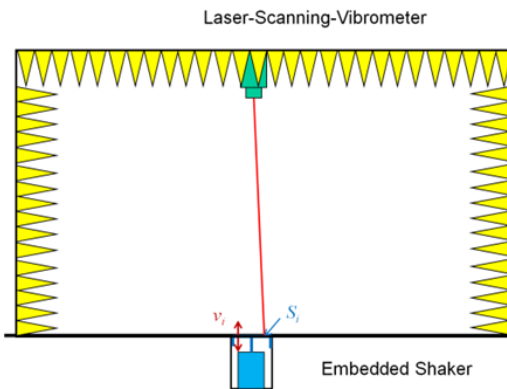


Figure 1 – Experimental set-up: Oscillating piston embedded in the floor of a hemi-anechoic room.

used during calculations can be traced to the SI units. Thus, this experimental set-up has the potential to serve as a primary realization of the unit Watt in airborne sound with the benefit that no measurements in the airborne sound field are necessary. The uncertainty level of the determined sound power output of the primary standard is expected to be around 0.5 dB (18). A first verification of the theoretical and experimental compatibility of this set-up and first analytical results were given in (17, 18, 19).

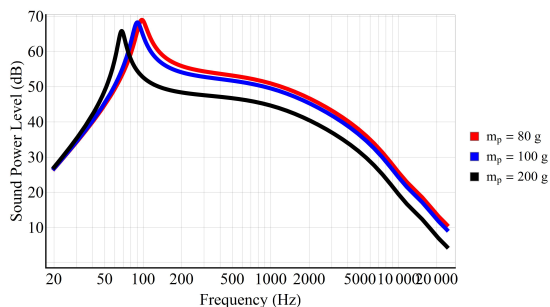
Once the sound power output with corresponding uncertainty budget of the primary standard has been established, a transfer standard for the dissemination of the unit Watt will be used. Aerodynamic reference sound sources are most likely to be used for broadband noise (20). However, a tonal transfer standard as well as the application of both transfer methods in the qualification of measurement set-ups and the determination of sound powers of real sound sources are further goals of the EMRP project (12).

### 3. PRELIMINARY STUDIES

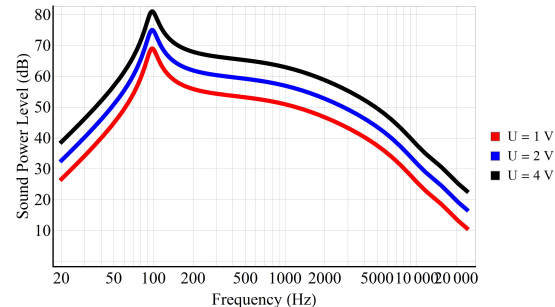
To assess the dimensioning and properties of possible pistons, a lumped parameter model was developed. This model allowed for a prediction of sound power output of the source depending on parameters such as

input voltage, piston mass, and radius of the piston. For construction and symmetry reasons, the piston was assumed to be circular.

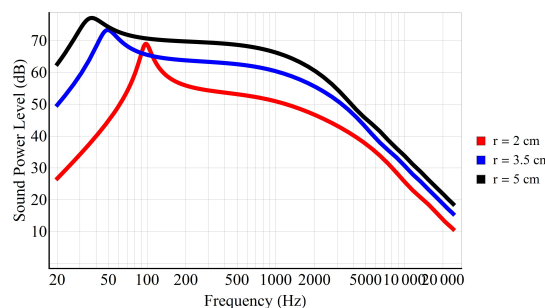
Results indicate that a larger piston mass leads to a decrease in sound power output (Fig. 2a) while an increasing input voltage leads to larger sound power levels for all frequencies (Fig. 2b). Smaller piston sizes lead to lesser sound power levels as well as a less flat frequency response than larger pistons. Furthermore, their first sound emission peak is at higher frequencies (Fig. 2c). But smaller piston sizes lead to a more uniform sound emission, which is desirable (Fig. 2d). Piston radii in excess of 5 cm should be avoided.



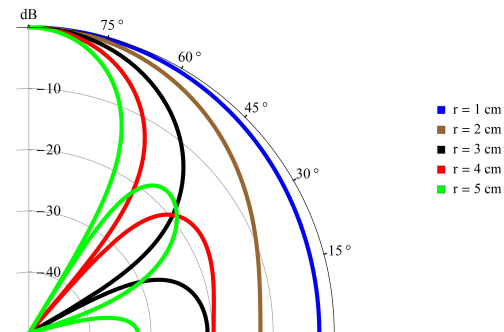
(a) Sound power level for different piston masses  $m_p$  with  $U = 1$  V (tonal) and  $r = 0.02$  m



(b) Sound power level for different voltages  $U$  (tonal) with piston radius  $r = 0.02$  m and  $m_p = 0.08$  kg



(c) Sound power level for different radii with  $U = 1$  V tonal excitation and  $m_p = 0.08$  kg



(d) Directivity of sound emission for different radii at  $f = 8$  kHz

Figure 2 – Variation of parameters

#### 4. EVOLUTION OF SOURCES

So far, six different pistons were used in experiments (Fig. 3). The different pistons used were:

- acrylic glass piston (Fig. 3a),
- piston of a combustion engine (Fig. 3b),
- aluminum piston (piston in the center - Fig. 3c),
- teflon (piston on the left - Fig. 3c),
- aluminum with teflon rings (piston on the right - Fig. 3c),
- and aluminum piston with silicon sealing (Fig. 3d).

Primary design restraints were that pistons had to be manufactured such that they could be embedded into the floor of a hemi-anechoic room with the piston surface forming a perfect alignment with the flooring. Also, the sound power output of the assembly was desired to be as large as possible and a temporal stability in the order of approximately an hour necessary for accurate measurements. Secondary design goals were the establishment of a flat frequency response and monopole-like sound emission.

Through step by step refinements source 6 was developed. It features an aluminum piston of radius  $r = 0.028$  m. The assembly is supported by a brass plate, where the space between brass plate and piston was filled with a silicon ring of  $l = 0.015$  m thickness (Fig. 3d). The refinements were necessary as the first five sources showed several deficiencies. First, their velocity and thus their sound power output were too small. Second, the frequency response of the vibration velocity was not flat (Fig. 4). And third, friction between the piston and the edges of the supporting plate caused non-linearities in the piston behavior and an excitation of the supporting plate by the moving piston.

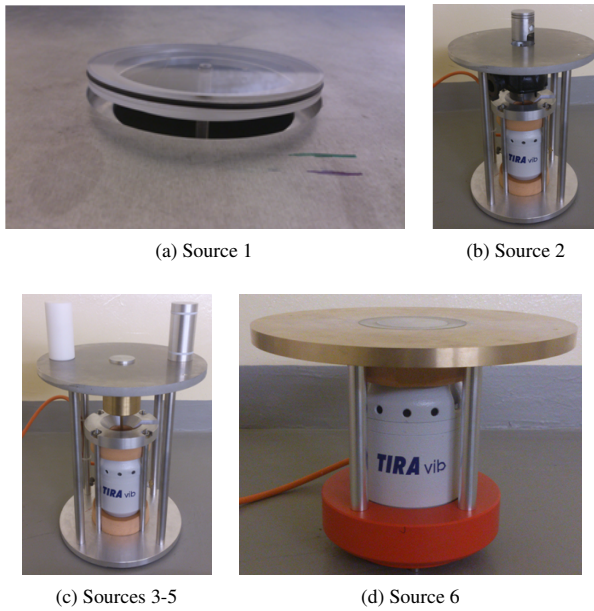


Figure 3 – Different pistons used for measurements

As source 6 shows the most promising results to this day, the following sections will give details on measurements and calculations carried out for that sound source.

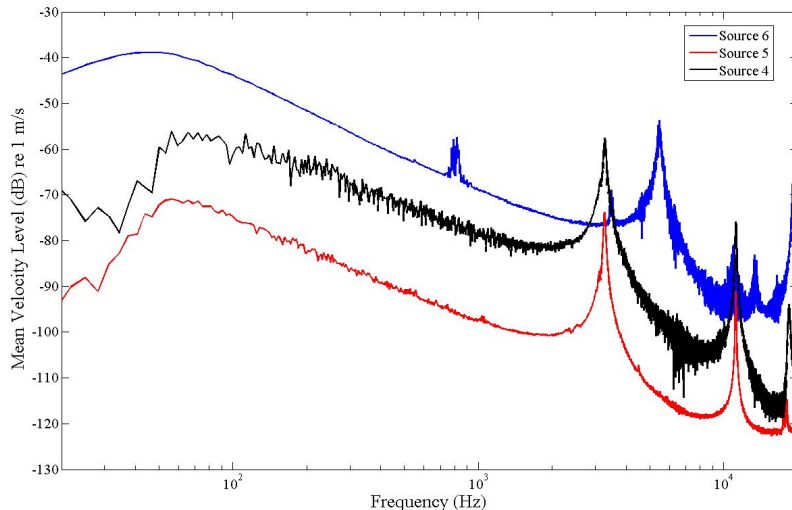


Figure 4 – Comparison of velocity levels for piston set-ups 4 to 6

## 5. MEASUREMENTS

Three sets of measurements were carried out. For all measurements source 6 was installed in a cavity of the floor of a hemi-anechoic room. During the first set of measurements a circular grid with 1425 measurement points including the piston, silicon ring, and part of the brass plate was defined and sampled by a laser scanning vibrometer. A multi-sine signal with 6400 lines and random phase was used in the range of 20 Hz to 20 kHz. Output data collected was the vibration velocity with corresponding phase in relation to the electrical input data. This data was used to calculate the sound power output using Rayleigh's integral.

The second measurement set was obtained from sound pressure measurements in the sound field, where a microphone was moved along a meridional path of the hemisphere surrounding the sound source. Sound pressure data were recorded in  $1^\circ$  steps for angles  $\alpha$  with  $0^\circ < \alpha \leq 90^\circ$ . The measurement was performed using a realtime one-third octave band analyzer where the excitation of the source was realized by the 6400

line multi-sine signal mentioned above. Assuming rotational symmetry this data was used to calculate the sound power output of the source (Fig. 9a) as well as to study the directivity of sound emission.

The third set of measurements utilised 24 1/2" microphones placed on a hemi circular metallic arc of 2 m radius. The arc was able to move over the primary source 6. During the measurements it was positioned at 5°, 15°, 25°, 35°, 45°, 55°, 65°, 75° and 85° angles with respect to the hemi-anechoic room floor. At each arc position, the time series of each microphone was recorded as a set of ten successive measurements of 20 second duration each, performed one right after another. After the recording a one-third octave band analysis was performed. The source was excited by the same signal as the previous measurements. These measurements will subsequently be referred to as "scanning measurements".

## 6. RAYLEIGH'S INTEGRAL

As introduced above, the first set of measurements was used to calculate the sound power emitted by source 6 using Rayleigh's integral (see Eq. 2). As measurement points included the piston, silicon ring, and part of the surrounding brass plate, sound power levels were calculated for the entire assembly as well as for the separate materials individually. Averaging the velocities of the measurement points on the piston surface, a comparison of the sound power of the actual piston to a theoretical rigid piston was carried out as well (Fig. 5).

Results indicate that the overall sound power output of source 6 is satisfactory for measurements in the sound field. This is important as sound pressure and/or intensity measurements will be needed for comparison to numerical results. Furthermore, the piston contributes the most to overall sound power. The silicon sealing is non-problematic for frequencies up to 800 Hz. However, its movement starts to become inhomogeneous after that point. Considering that its contribution to overall sound power is not significant for frequencies higher than 800 Hz, this is not a major complication, though. The first peak in sound power output occurs at 5.45 kHz with two minor peaks at 803 Hz and 3.49 kHz. These do not represent natural modes but are rather due to the constructional design of the source. As desired, the brass plate does not contribute significantly to the overall sound power output of the source (Fig. 5a). Comparing the sound power output of the actual piston to a rigid piston shows a good agreement up to 7 kHz which indicates that the piston movement is very uniform up to that point (Fig. 5b).

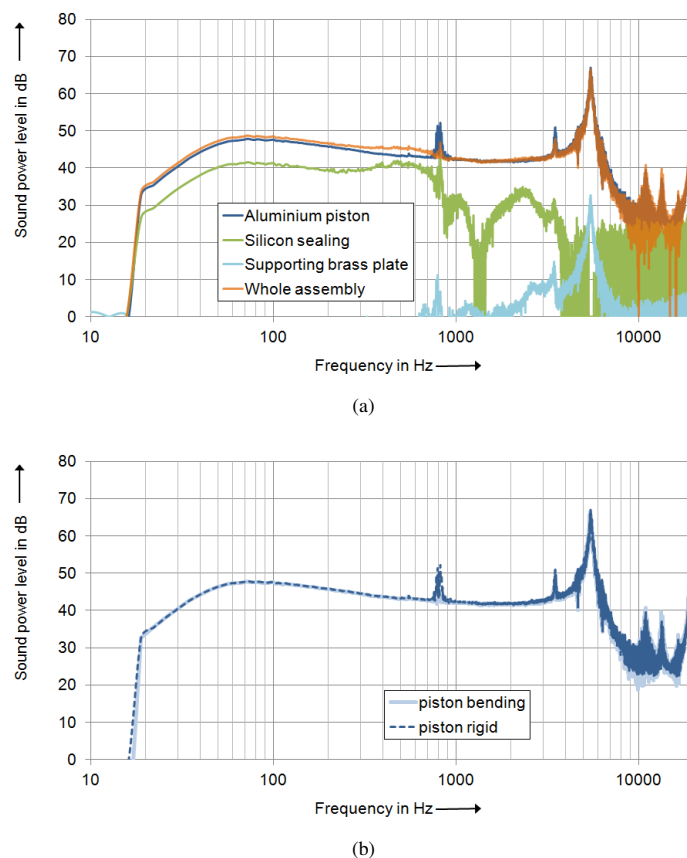


Figure 5 – Sound power levels calculated using Rayleigh's integral

To perform an initial assessment of the dependency of calculated results on the number of measurement points used, calculations were repeated for the same set-up using only every second data point of the original data set. Thus, the number of measurement points of the original set (1425 points) was reduced to 713 data points (see Fig. 6). Results indicate that the piston surface is sufficiently discretized using the smaller grid for frequencies up to 7 kHz (Fig. 7a). However, sound power levels of the silicon sealing surrounding the piston differ significantly for frequencies higher than 800 Hz (Fig. 7b). Considering the previously mentioned inhomogeneity of its movement for higher frequencies, this is expected. But it does mean that the question of necessary discretization is unanswered for the silicon sealing at this point.

Due to the large differences in computed sound power levels for the silicon sealing, the calculated sound power level of the complete set-up shows large deviations for higher frequencies as well (Fig. 7c). Looking at the differences in sound power levels themselves confirms the large fluctuations for the silicon sealing. But, it is also visible that the sound power levels calculated for the piston start to vary by up to 2 dB for frequencies higher than 7 kHz (Fig. 7d). This corresponds to the previous result indicating that the piston does not move uniformly for larger frequencies.

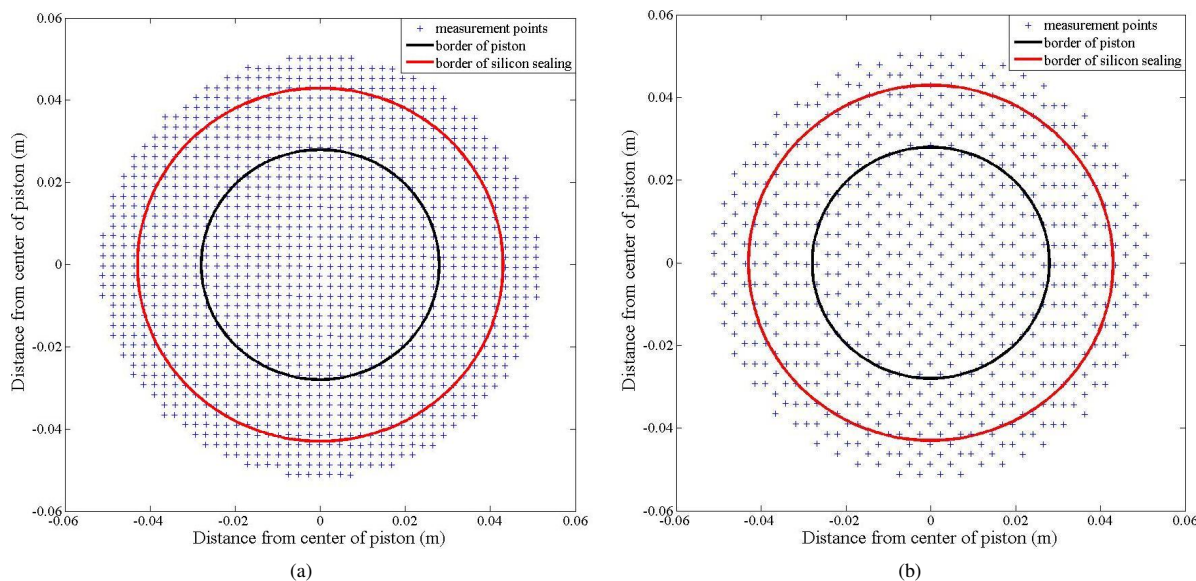


Figure 6 – Comparison of grids used for calculations

## 7. NUMERICAL STUDIES

Numerical simulations using finite element software were performed for source 4 and frequencies up to 300 Hz. Measurement data for that source included 37 data points on the piston surface. These were modeled and their frequency-specific measured velocities prescribed for the simulation. Output data collected included sound pressure, particle velocity and intensity values along a meridional arc of radii ranging from 0.5 m to 3.0 m in steps of 0.5 m for angles of 0° to 90° in steps of 1.5°.

The goal of these first numerical studies was to determine whether the source under test behaved like a monopole. This was accomplished by investigating:

1. Does the sound power calculated from sound pressure data equal that from sound intensity data?
2. Is sound emission uniform?
3. Does the angle between the sound pressure and the radial component of the particle velocity correspond to the theoretical value of a monopole?

Future numerical studies will additionally investigate whether the calculated sound power levels of the numerical model match the values calculated via Rayleigh's integral.

Results on the first question indicate very good agreement between sound power levels from pressure and intensity data. In fact, in the frequency range investigated the maximum difference in sound power levels is 0.02 dB. Comparing these sound power levels to those of a rigid piston (using the average measured velocity on the piston surface as input) shows a deviation of less than 1 dB to both sound pressure and sound intensity based SWL calculations.

Results on the second question show that the sound emission for the source under test is very uniform (Fig. 8a). To further confirm the monopole-like behavior of source 4, the difference between the phase angles of

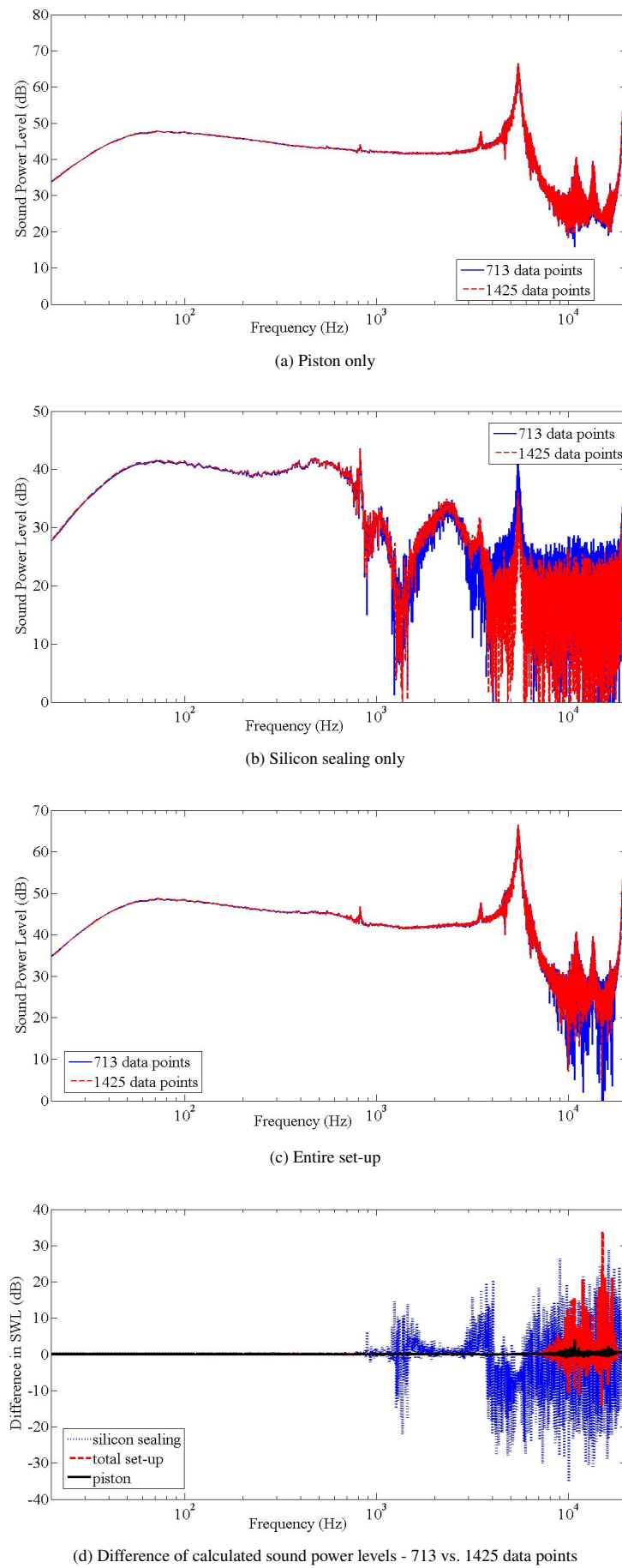


Figure 7 – Comparison of calculated SWL using two different grids for indicated areas

sound pressure and particle velocity was computed. This value was compared to the theoretical value of a monopole as given by Eq. 3 (15).

$$\angle(p, v_r) = -\arctan\left(\frac{1}{kr}\right) \quad (3)$$

It can be seen that the absolute value of the difference between the numerical and theoretical value stays below  $0.4^\circ$  for the investigated frequency range with the largest differences occurring for the largest frequency observed (300 Hz) (Fig. 8b). That trend could be due to the mesh used for simulations and/or sound emission being not entirely uniform for that frequency anymore. Nevertheless, an absolute deviation of less than  $0.4^\circ$  together with the previous results indicates that the source under test behaves like a monopole. Retaining this trait for future sources is important as sound power levels of monopole sources can be accurately measured using sound pressure microphones at any distance from the source (16).

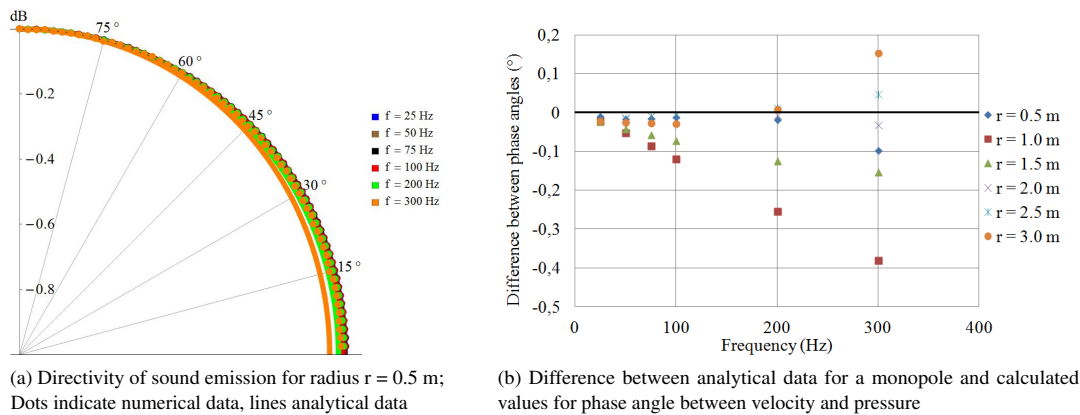


Figure 8 – Numerical results for directivity and near field effect

## 8. COMPARISON OF RESULTS FROM DIFFERENT METHODS

Two different comparisons were carried out:

1. Using the data from sound pressure and scanning measurements of source 6 as well as those calculated from Rayleigh's integral, a comparison between the sound power levels was carried out. Deviations below 63 Hz can be attributed to the hemi-anechoic room used for measurements. Between 63 and 500 Hz there is very good agreement between pressure measurement results and Rayleigh's integral data. Sound power levels from the scanning measurements deviate by approximately 2 dB from the other two methods (Fig. 9a). Beyond 500 Hz sound power level differences between pressure measurements and Rayleigh's integral exceed 4 dB (Fig. 9b). These discrepancies could be in part due to the sensitivity of the Rayleigh's integral results on discretization as described previously. However, other and up to this point unknown effects are likely to play a role, too. Considering that the scanning measurements fit the Rayleigh's integral results much better than the pressure measurement results beyond 500 Hz, the realization of the unit Watt still seems possible for those frequencies (Fig. 9b).
2. The second comparison between measurements and calculations concerned the directivity data obtained from the pressure measurements. These data were compared to analytical predictions calculated for the preliminary studies (see Fig. 2d). For the analytical calculations solely the piston without the silicon sealing was modeled as previous results showed that the piston is the major contributor to the sound power output. Results indicate that the sound emission is very uniform and that the analytical model fits the measurement data very well up to 1.25 kHz (Fig. 10a). At 2.5 kHz the sound emission is approximately 1 dB larger in the  $90^\circ$  than in the  $0^\circ$  direction and small differences between analytical and measurement results become visible (Fig. 10b). For frequencies higher than 2.5 kHz the differences between both methods become larger. However, both analytical as well as measurement results display the same trend towards larger sound emission in the  $90^\circ$  direction (Fig. 10c). At 10 kHz analytical and measurement data display a second sound emission peak. At this point, the general behavior of the curves generated by both methods is similar. However, the absolute difference between the results of the two methods becomes significant (Fig. 10d). Looking at the sound power analysis performed previously (Fig. 5a) this is expected, though. From 8 kHz onward the movement of the silicon sealing is erratic and the piston surface starts to show non-uniform motion as well. As the analytical model cannot

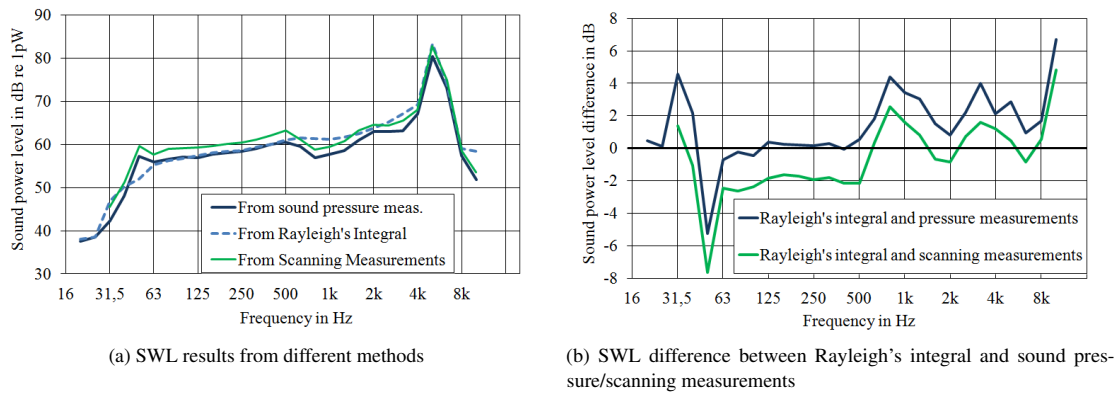


Figure 9 – Comparison of sound power levels: Measurements and calculation using Rayleigh's integral

accommodate for this behavior it is satisfactory to observe that both analytical as well as measurement data agree in their qualitative description of sound emission even if there are quantitative differences between both methods.

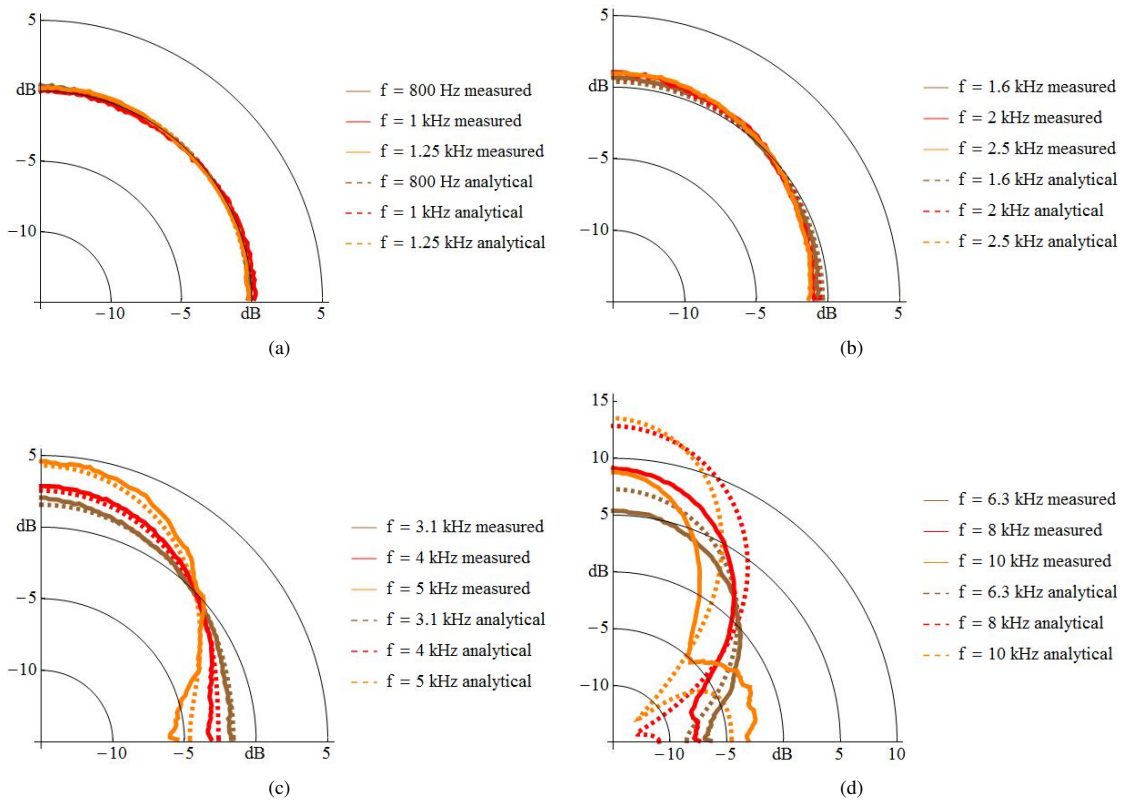


Figure 10 – Directivity of sound emission for different frequencies

## 9. CONCLUSION

This contribution reported on the first results of an EMRP project trying to establish a realization of the unit Watt in airborne sound. Using three approaches to determine the sound power output of a source - measurements in the sound field, Rayleigh's integral, and numerical simulations - a primary standard is to be developed. The most recent set-up shows very promising results and future goals include a refinement of the source as well as a determination and verification of its sound power output including an uncertainty budget of less than 0.5 dB.

The work presented in this paper is part of the EMRP joint research project SIB56 'Sound power'. The EMRP is jointly funded by the EMRP participating countries within EURAMET and the European Union.

## REFERENCES

1. European directive 2000/14/EC "Outdoor Directive"
2. European directive 2006/42/EC "Machinery Directive"
3. European directive 2010/30/EU "Energy Labeling Directive"
4. ISO 3745 Acoustics – Determination of sound power levels and sound energy levels of noise sources using sound pressure – Precision methods for anechoic rooms and hemi-anechoic rooms, 2012
5. ISO 3744 Acoustics – Determination of sound power levels and sound energy levels of noise sources using sound pressure – Engineering methods for an essentially free field over a reflecting plane, 2010
6. ISO 3746 Acoustics – Determination of sound power levels and sound energy levels of noise sources using sound pressure – Survey method using an enveloping measurement surface over a reflecting plane, 2010
7. ISO 3741 Acoustics – Determination of sound power levels and sound energy levels of noise sources using sound pressure – Precision methods for reverberation test rooms, 2010
8. ISO 3743-2 Acoustics – Determination of sound power levels of noise sources using sound pressure – Engineering methods for small, movable sources in reverberant fields – Part 2: Methods for special reverberation test rooms, 1994
9. ISO 9614-1 Acoustics – Determination of sound power levels of noise sources using sound intensity – Part 1: Measurement at discrete points, 1993
10. ISO 9614-2 Acoustics – Determination of sound power levels of noise sources using sound intensity – Part 2: Measurement by scanning, 1996
11. ISO 9614-3 Acoustics – Determination of sound power levels of noise sources using sound intensity – Part 3: Precision method for measurement by scanning, 2002
12. Wittstock, V.: A new approach in sound power metrology. OIML Bulletin Vol. 55 Number 2/3 (2014), 9-13
13. Hübner, G.: Eine Betrachtung zur Physik der Schallabstrahlung. Acustica Vol. 75 (1991), 130-144
14. Hübner, G.; Gerlach, A.: Zusammenhang der DFEM-Schallleistungsbeschreibung mit der Rayleighschen Schallfelddarstellung ebener Strahler. Proc. of DAGA 1998, Zurich (1998), 682-683
15. Fasold, W., Kraak, W., Schirmer, W.: Taschenbuch Akustik Teil 1. VEB Verlag Technik Berlin, Berlin (1984), 35-36
16. Hübner, G.: Analysis of errors in measuring machine noise under free-field conditions. The Journal of the Acoustical Society of America 54 (1973), 967-977
17. Schmelzer, M., Wittstock, V., Bethke, C.: Numerical computation and experimental verification of the emitted sound power of a vibrating baffled piston into a hemi-anechoic room. AIA-DAGA 2013, Proceedings of the International Conference on Acoustics (2013), 1987-1990
18. Wittstock, V., Schmelzer, M., Bethke, C.: Establishing traceability for the quantity sound power. Proceedings of Internoise 2013, 42nd International Congress and Exposition on Noise Control Engineering, Innsbruck, Austria, 2013
19. Völkel, K., Schmelzer, M., Wittstock, V.: Analytical and Numerical Investigation of the Sound Power Emission of a Vibrating Baffled Piston Into a Hemi-Anechoic Room. Proceedings of DAGA 2014 on CDROM, Oldenburg, Germany, 2014
20. Brezas, S.; Wittstock, V.: Properties of aerodynamic reference sound sources. Proceedings of DAGA 2014 on CDROM, Oldenburg, Germany, 2014